

# Comparison of far-infrared properties of high-ionization broad absorption line AGN and general quasar population

L.K. Pitchford<sup>1,2\*</sup>, E. Hatziminaoglou<sup>1</sup>, D. Farrah<sup>2</sup>, A. Feltre<sup>3</sup>

<sup>1</sup>ESO, Karl-Schwarzschild-Str. 2, 85748 Garching bei München, Germany

<sup>2</sup>Department of Physics, Virginia Tech, Blacksburg, VA 24061, USA

<sup>3</sup>Institut d'Astrophysique de Paris, 98 bis boulevard Arago, 75014 Paris, France

\*Email: lpitchfo@eso.org



## Abstract

Using a sample of  $\sim 600$  quasars detected by the Sloan Digital Sky Survey (SDSS), as well as the Spectral Imaging and Photometric Imaging Receiver (SPIRE) instrument of *Herschel*, we aim to describe the behavior of bright quasars in the far-infrared (FIR) and how it correlates with the properties intrinsic to the active galactic nucleus (AGN).

To achieve this, we use a spectral energy distribution (SED) fitting technique to quantify the FIR emission of our objects, as this wavelength probes the cold dust heated by star formation. As such, we can easily extract the star formation rates (SFRs) of these host galaxies from the output of the SED fit. Our sample includes 47 high-ionization broad absorption line quasars, which we study with particular care to ascertain whether the SFRs in their respective host galaxies deviate from those of the hosts of quasars that do not exhibit broad absorption lines (BALs) in their spectra.

## Sample

Our sample compiles all of the quasars detected by SDSS, whether in data release (DR) 7 or 10 [1, 2], and two large *Herschel* fields, HerMES and HerS [3, 4]; we cross-match these catalogues using  $15''$  matching radius. We further stipulate that all objects must have a  $3\sigma$  detection at  $250 \mu\text{m}$ . The resultant quasar population contains 195 quasars in the HerMES fields and 369 objects located in HerS.

In addition to the optical and FIR data provided by SDSS and SPIRE, we have some near- and mid-infrared data from 2MASS, UKIDSS, and WISE [5, 6, 7]. There are 184 objects with WISE data, 88 with 2MASS data, and 332 with data from UKIDSS.

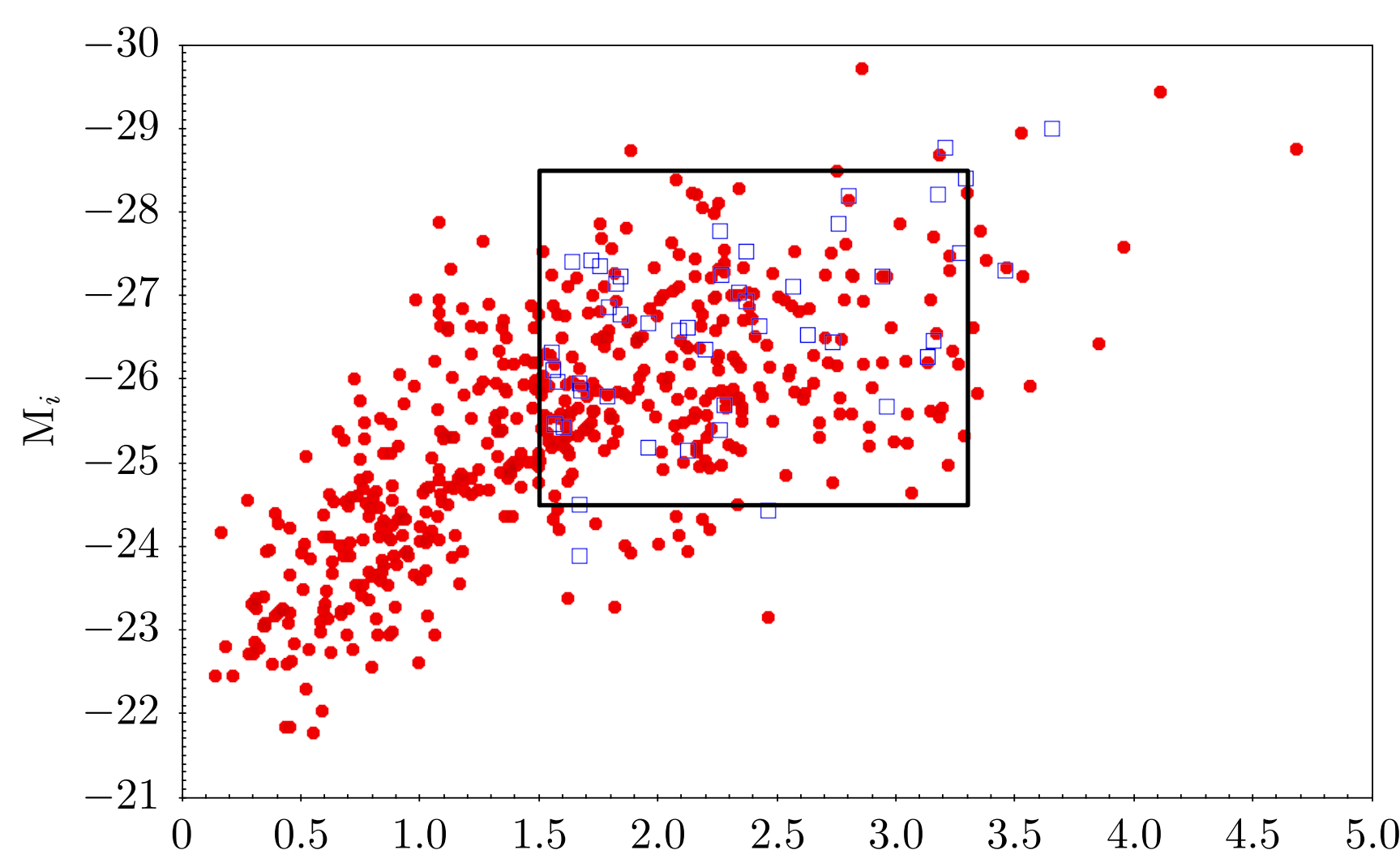


**Figure 1:** Absolute *i*-band magnitude versus redshift. The open squares are the HiBAL quasars, while the filled circles represent the non-BAL quasar population. We choose to focus our analyses on the objects inside the black box (288 quasars); the cuts in absolute magnitude and redshift are made to encompass the majority of our BAL sample.

## BAL quasars

To determine our BAL sample in order to study any differences between it and the non-BAL quasar population, we rely on the SDSS BAL flag. Our sample includes 49 BAL quasars; however, 47 are of the high-ionization (HiBAL) classification, while 2 are low-ionization BAL (LoBAL) quasars. Because of potential differences among the two classifications, we choose to exclude the 2 LoBAL quasars from our sample. Both populations (HiBAL and non-BAL) are detected at  $\sim 10\%$  ( $\frac{47}{408}$  for the HiBAL quasars and  $\frac{515}{4905}$  for the non-BAL population).

## SED fitting

The emission from each of our quasars can be described using their respective SEDs [8, 9]. Due to the redshifts covered by our sample, we choose to neglect the stellar component of the fit, as our quasars should be sufficiently bright so as to outshine their hosts; as such, all of our objects' emission can be attributed to either an AGN or a starburst component.

**Input:** The SED fitting technique operates using flux measurements, along with their associated errors, in completing the fit. We choose to fit the AGN component using a simplified set of smooth torus models and the starburst component with one of six templates; for the full set of torus models, see Feltre et al. 2012 [10].

**Output:** Example fits are given below. From the code's output, we have the bolometric luminosity due to accretion, which is used to find the Eddington ratio, as well as the FIR luminosity from which the host SFR is derived.

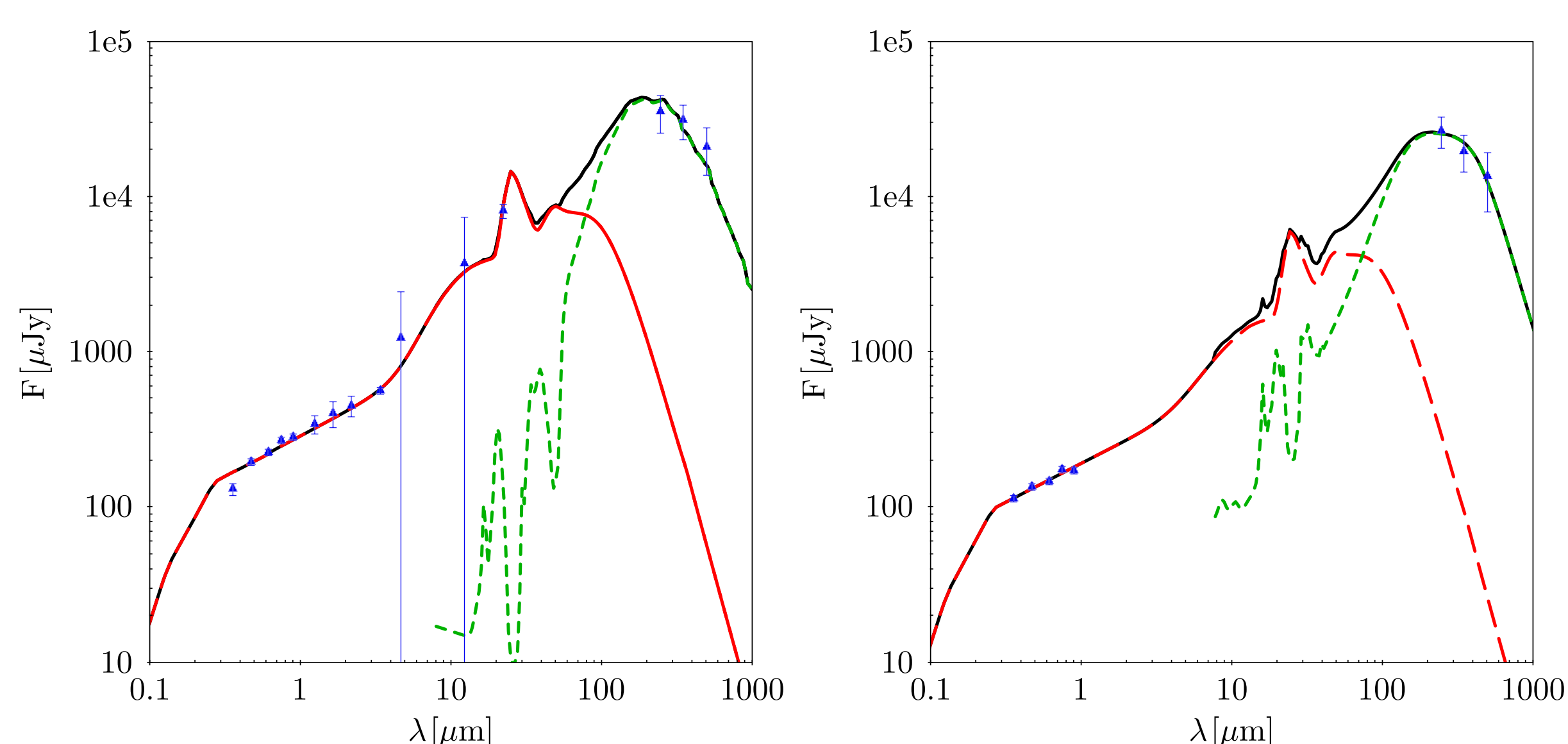


**Figure 2:** Example SED fits. The solid, black line represents the total fit; the red, dashed line shows the AGN component, while the green, dotted line is that of the starburst. The plot on the left is a BAL quasar, while that on the right is a non-BAL quasar.

## Results

**SFR:** We can easily calculate the SFRs associated with the host galaxies of each of our quasars using the relation first described by Kennicutt et al. 1998 [11]:

$$\frac{SFR}{M_{\odot} \text{yr}^{-1}} = 4.5 \times 10^{-44} \times \frac{L_{SB}}{\text{erg s}^{-1}}$$

where  $L_{SB}$  is the luminosity of the starburst component, integrated between 8 and  $1000 \mu\text{m}$ . The distributions of the SFRs in both the BAL and non-BAL sample are found to be roughly the same and are given in Figure 3.

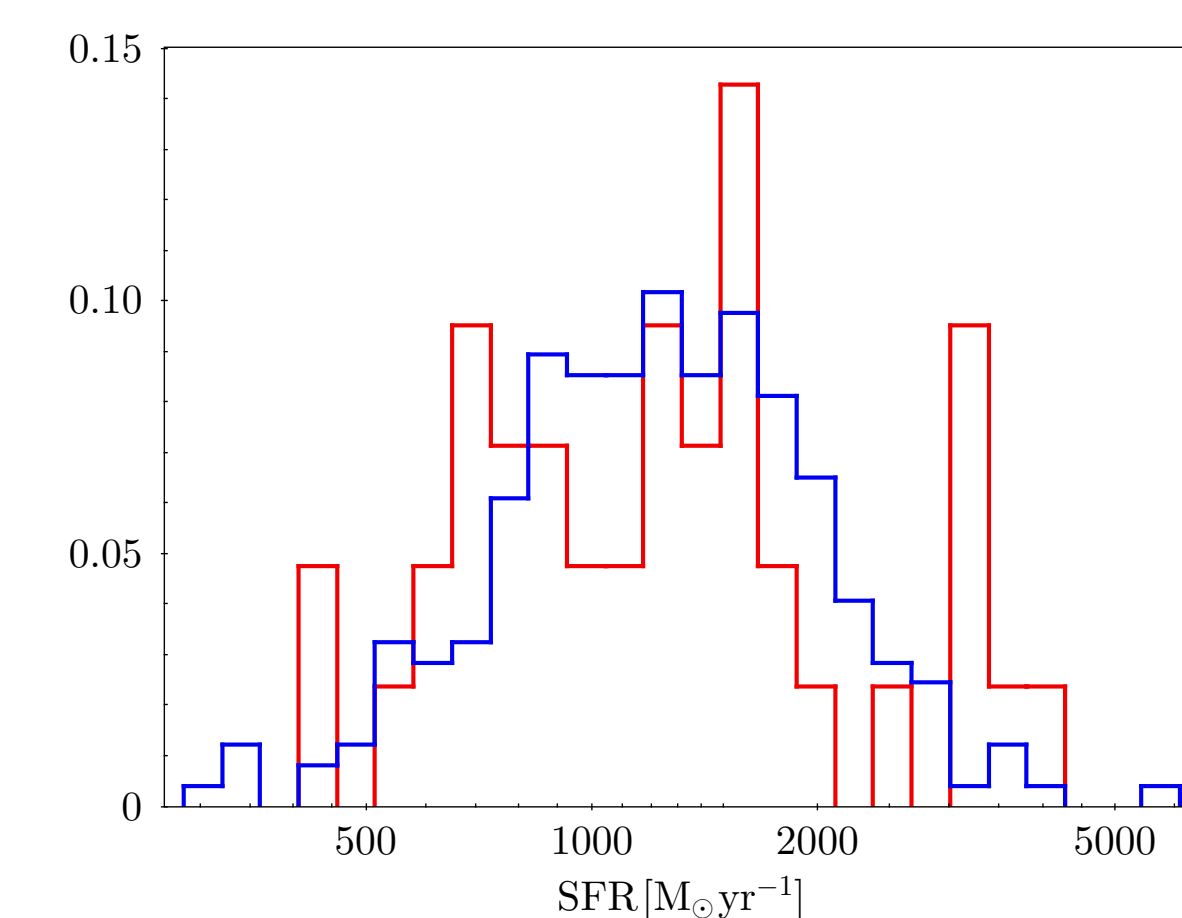


**Figure 3:** SFR distributions for objects with  $1.5 < z < 3.3$ . The red outline shows the SFRs of those host galaxies of BAL quasars, while the blue outline describes the hosts of quasars that do not exhibit BALs in their spectra. The presence of BALs in quasar spectra, therefore, does not seem to affect the host.

$$BAL : 1251.13 \pm 698.006 [M_{\odot} \text{yr}^{-1}]$$

$$non-BAL : 1232.26 \pm 595.437 [M_{\odot} \text{yr}^{-1}]$$

**Black Hole Mass:** Using the emission line measurements provided by SDSS, we can calculate the mass of the black hole powering each quasar; the SFR as a function of  $M_{BH}$  is given in Figure 4.

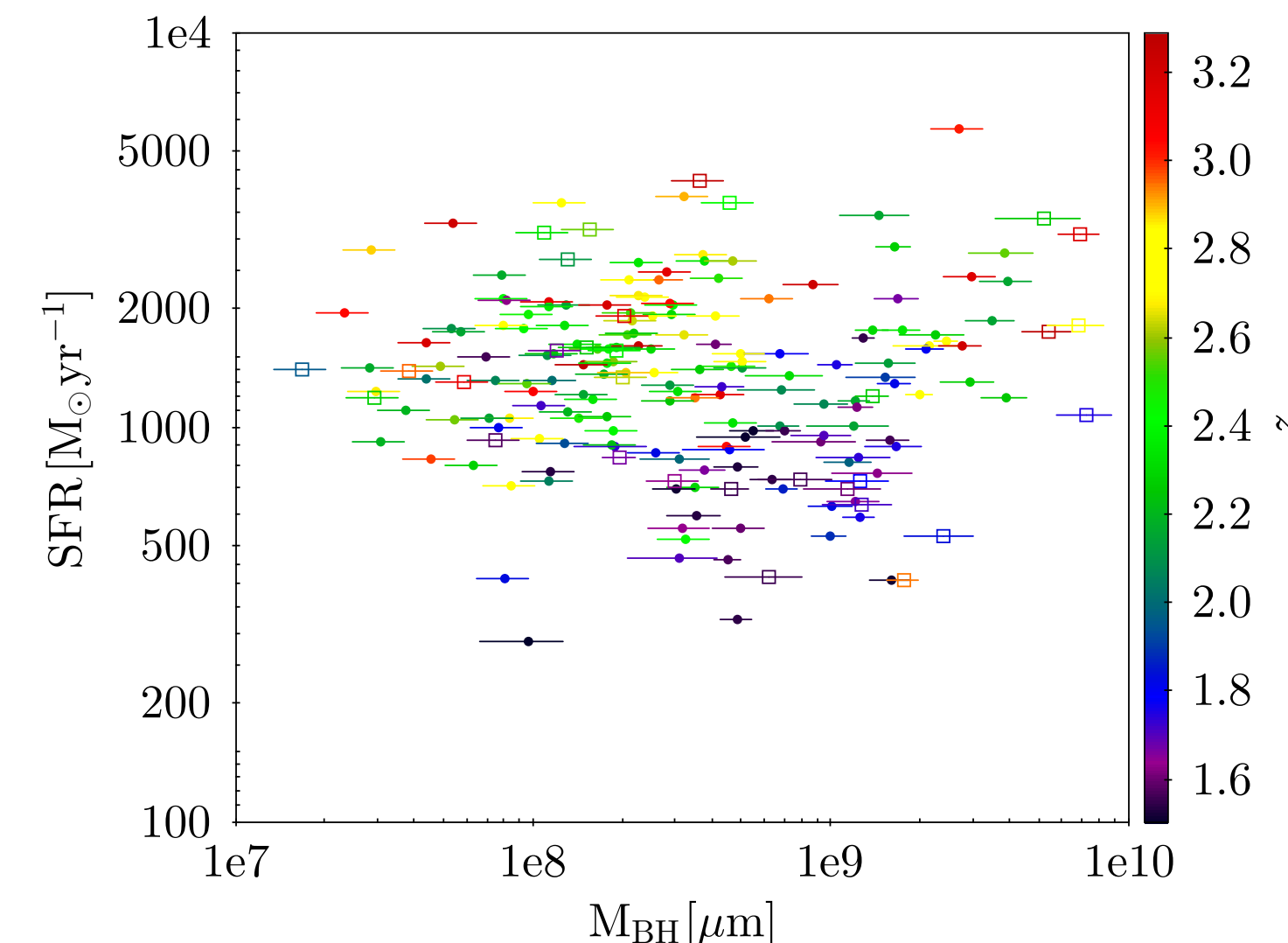


**Figure 4:** SFR versus black hole mass color-coded by redshift. The open squares are the BAL objects, while the closed circles are the non-BAL quasars. The two samples seem to behave in the same manner.

To determine whether the increasing SFR is due to an absolute magnitude or a redshift evolution, we are currently in the process of binning our objects in these two quantities and studying how the mean SFR changes within each bin.

**Eddington Ratio:** Using our black hole mass estimates, we can additionally calculate the Eddington ratio,  $\lambda_{Edd}$ , associated with each black hole; the SFR as a function of this ratio is shown in Figure 5.

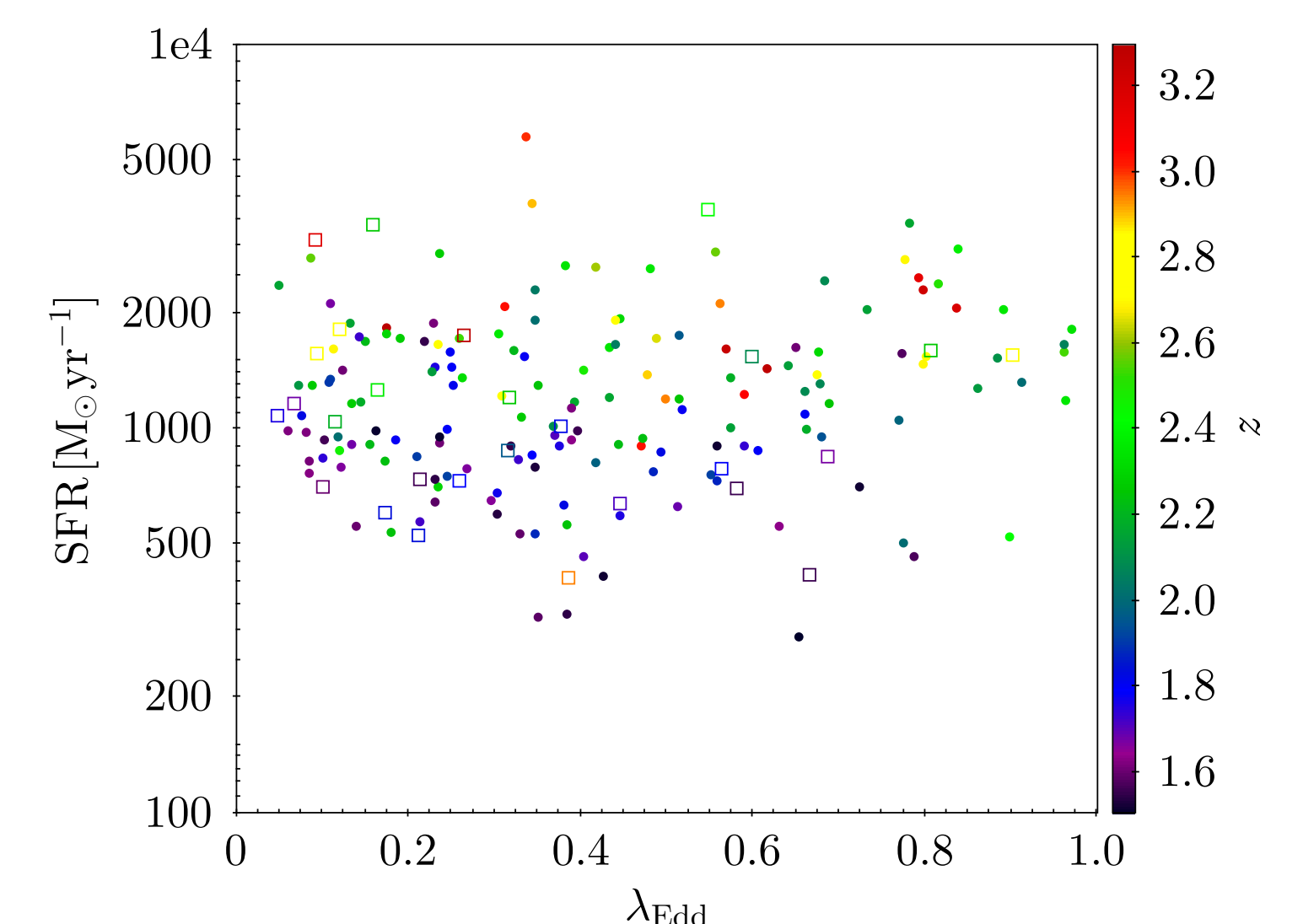


**Figure 5:** SFR versus Eddington ratio color-coded by redshift. The shapes are the same as described in Figure 4. Again, there is no distinction between the HiBAL sample and the non-BAL counterpart.

## Conclusions

The BAL quasars seem to share the same characteristics as their non-BAL counterparts; they have the same optical properties, detection rates, and SFRs as do those quasars that do not exhibit BALs in their spectra. As such, we conclude that the difference between the two types is indeed due to an orientation effect.

## References

- [1] Schneider D. P. et al. 2010, AJ, 139, 2360
- [2] Pâris I. et al. 2014, A&A, 563, AA54
- [3] Oliver S. et al. 2012, MNRAS, 424, 1614
- [4] Viero M. P. et al. 2014, ApJS, 210, 22
- [5] Skrutskie M. F. et al. 2006, AJ, 131, 1163
- [6] Lawrence A. et al. 2007, MNRAS, 379, 1599
- [7] Wright E. L. et al. 2010, AJ, 140, 1868
- [8] Hatziminaoglou E. et al. 2008 MNRAS, 386, 1252
- [9] Hatziminaoglou E., Fritz J., Jarrett T. H. 2009, MNRAS, 399, 1206
- [10] Feltre A., Hatziminaoglou E., Fritz J., Franceschini A. 2012, MNRAS, 426, 120
- [11] Kennicutt R. C., Jr. 1998, ARA&A, 36, 189